

Supporting Information

Interface molecular wires induce electron transfer from COFs to Pt for enhanced photocatalytic H₂ evolution

Zhengfeng Zhao^{a*}, Weiqiang Chen^b, Guofeng Zhang^a, Yao Chen^{c*}

^aSchool of Chemistry and Chemical Engineering, Qilu University of Technology (Shandong Academy of Sciences), Jinan 250353, China

^bLONGi Solar Technology Co., Ltd, Xi'an 710018, China

^cState Key Laboratory of Medicinal Chemical Biology, College of Pharmacy, Nankai University, Tianjin 300071, China

Corresponding Author

zzf@qlu.edu.cn(mse_zhengfengzhao@163.com) ;chenyao@nankai.edu.cn.

1. Materials and Methods

General. All materials were commercially available and used without further purification. All solvents were of analytical grade and used without further purification. 2,4,6-trihydroxybenzene-1,3,5-tricarbaldehyde (Tp, Jilin Chinese Academy of Sciences-Yanshen Technology Co., Ltd (ET Co.,Ltd)), Benzene-1,4-diamine (Pa, Aladdin), Glacial acetic acid, sodium citrate, mesitylene, 1,4-Dioxane were purchased and used without further purification.

Characterization. PXRD patterns of all the materials were collected at ambient temperature on Rigaku Dmax 2500 diffractometer using Cu K α ($\lambda=1.5418$ Å) radiation, and a 2θ range of 1.5° to 30° . Fourier transform infrared spectra (FT-IR) were recorded on Nicolet IS10. X-ray photoelectron spectroscopy (XPS) and ultraviolet photoelectron spectroscopy (UPS) measurements were performed on an X-ray photoelectron spectrometer (Thermo Scientific ESCALAB Xi+). Low-pressure gas adsorption measurements were measured with BELSORP MaxII for surface area and pore size analysis. A liquid nitrogen bath was used for the N₂ measurements at 77 K. UV-vis diffused reflectance spectra were measured on a UV spectrophotometer (UV-2700, Shimadzu). Steady-state photoluminescence (PL) and excited-state decay spectra were measured on FLS1000-Edinburgh Instruments. Photoelectrochemical characterization was carried out on a CHI600E workstation. Transmission electron microscopy (TEM, JEOL-JEM 2100 F) was used to analyze the morphologies of the PtNPS and the photocatalysts.

Structure simulations:

Structural modeling of all the NKCOFs was generated using the Accelrys Materials Studio software package. The lattice model was geometry optimized using the Forcite module. Pawley refinement was applied to define the lattice parameters.

Synthesis of CTF-1¹. In a typical experiment, 400 mg terephthalonitrile (DCB) and 200 μ L CF₃SO₃H were added to a pyre ampoule. The ampoule was evacuated, flame-sealed, and heated to 200 °C in a muffle furnace for 48 h. Then the obtained solid was washed with tetrahydrofuran in a Soxhlet extractor for 24 h to thoroughly remove the unreacted monomer. Then TpPa-1 was dried under vacuum at 80 °C.

Synthesis of CYANO-COF². A 10 mL high-pressure flask was charged with Tp (21 mg, 0.1 mmol) and 4,4'-diamino-[1,1'-biphenyl]-3,3'-dicyanitrile (35.1 mg, 0.15 mmol). A mixture of 0.5 mL 1,4-dioxane 0.5mL mesitylene and 0.25 mL aqueous acetic acid (6M) was added. The flask was degassed through three freeze-pump thaw cycles to remove any dissolved oxygen. After warming it to room temperature, the flask was charged with N₂, sealed under positive N₂ pressure, and then placed into a 120 °C pre-heated oil bath for 3 days. After that, the obtained solid was washed with DMF, acetone, and THF for several times and extracted by Soxhlet extraction using THF for 1 day. Finally, the solid materials were dried under vacuum at 80 °C overnight to get the CYANO-COFs in ~80% isolated yield.

Synthesis of NKCOF-113-M³. A 10 mL pyrex tube was charged with 2,4,6-Tris(4-formylphenyl)-1,3,5-triazine (TA-1Ph-CHO) (12.6 mg, 0.032 mmol), 5,5'-bis(cyanomethyl)-2,2'-bipyridine (BPy-CN) (11.3 mg, 0.048 mmol) and benzoic anhydride (22.5 mg, 0.1 mmol). This mixture was degassed through three freeze-pump-thaw cycles, and sealed under a vacuum. Then the tube was transferred into an oven to heat at 200 °C for 3 days yielding a yellow solid that was washed with tetrahydrofuran and methanol in a Soxhlet extractor for 48 h (yield ~95%). **NKCOF-113-M** was then activated by drying under vacuum at 80 °C for 12 h.

Synthesis of PtNPs (PVP)⁴. 0.1 mL H₂PtCl₆ aqueous solution (50 mM) was measured in the Schlenk tube, and 50 mg polyvinyl pyrrolidone (PVP), and 5 mL anhydrous ethylene glycol, were added into the above solution. The mixture solution was sonicated for 5 min and then vacuumed. The vacuum tube containing the mixed solution was heated with an oil bath at 120 °C until the solution turned brownish yellow and cooled to room temperature to obtain PtNPs (PVP). Subsequently, an appropriate amount of the solution was precipitated with acetone and then collected by centrifugation at 8000 rpm for 5 min. Then the sample was washed with acetone and hexane to remove excess free PVP and then redispersed in 5 mL water.

Electrochemical measurements: The Pt flake and Ag/Ag⁺ electrodes were used as counter electrode

and reference electrode, respectively. The solution of 0.1 M tetrabutylammonium hexafluorophosphate (TBAPF₆) in CH₃CN was prepared for the supporting electrolyte. Ferrocenium/ferrocene (Fc/Fc⁺) redox potential was measured at the end of each experiment to calibrate the pseudo reference electrode. The CV curves were tested with a scan rate of 0.05 V/s. The conduction band (CB) was calculated from the onset potentials of reduction and by assuming the energy level of ferrocene/ferrocenium (Fc/Fc⁺) to be -4.8 eV below the vacuum level.⁵⁻⁷ The valence band (VB) was determined to the related CB energy levels and band gap (E_g). The VB and CB levels are determined as follows:

$$E_{CB} = -[E_{red} - E_{1/2} + 4.8] \text{ eV and}$$

$$E_{VB} = E_{CB} - E_g.$$

E_{red} corresponds to the onset reduction potentials obtained from the tangents in CV.

E_g was determined from the UV/Vis diffuse reflectance spectra.

E_{1/2} is the redox potential of ferrocene/ferrocenium (Fc/Fc⁺) couple for the calibration (Fig.S16), E_{1/2} = (E_{ox}(Fc/Fc⁺) + E_{red}(Fc/Fc⁺))/2.

The apparent quantum yield (AQY) measurements:

The apparent quantum yield (AQY) for H₂ evolution was measured using monochromatic LED lamps with bandpass filters of 420 ± 10 nm, 450 ± 10 nm, 475 ± 10 nm, 500 ± 10 nm, 550 ± 10 nm, and 600 ± 10 nm (ILT 950 spectroradiometer). For the experiments, 0.5%PtNPs-TpPa-1 (10 mg) was suspended in an aqueous solution containing ascorbic acid (0.1 M). The irradiation area was controlled as 3.14 × 2.8² cm². The AQY was calculated according to the following Eq.:

$$\begin{aligned} \eta_{AQY} &= \frac{N_e}{N_p} * 100\% \\ &= \frac{2 * M * N_A}{\frac{E_{total}}{E_{photon}}} * 100\% \\ &= \frac{2 * M * N_A}{\frac{S * P * t}{h * \frac{c}{\lambda}}} * 100\% \end{aligned}$$

$$= \frac{2 * M * N_A * h * c}{S * P * t * \lambda} * 100\%$$

Where N_e is the amount of generated electrons for H_2 , N_p is the amount of incident photons, M is the amount of H_2 molecules (mol) during 1 hour, N_A is Avogadro constant ($6.022 \times 10^{23} \text{ mol}^{-1}$), h is the Planck constant ($6.626 \times 10^{-34} \text{ J}\cdot\text{s}$), c is the speed of light ($3 \times 10^8 \text{ m/s}$), S is the irradiation area (m^2), P is the intensity of irradiation light (W/m^2), t is the photoreaction time ($\text{s}=3600 \text{ s}$), λ is the wavelength of the monochromatic light (m).

2. Supporting tables and figures.

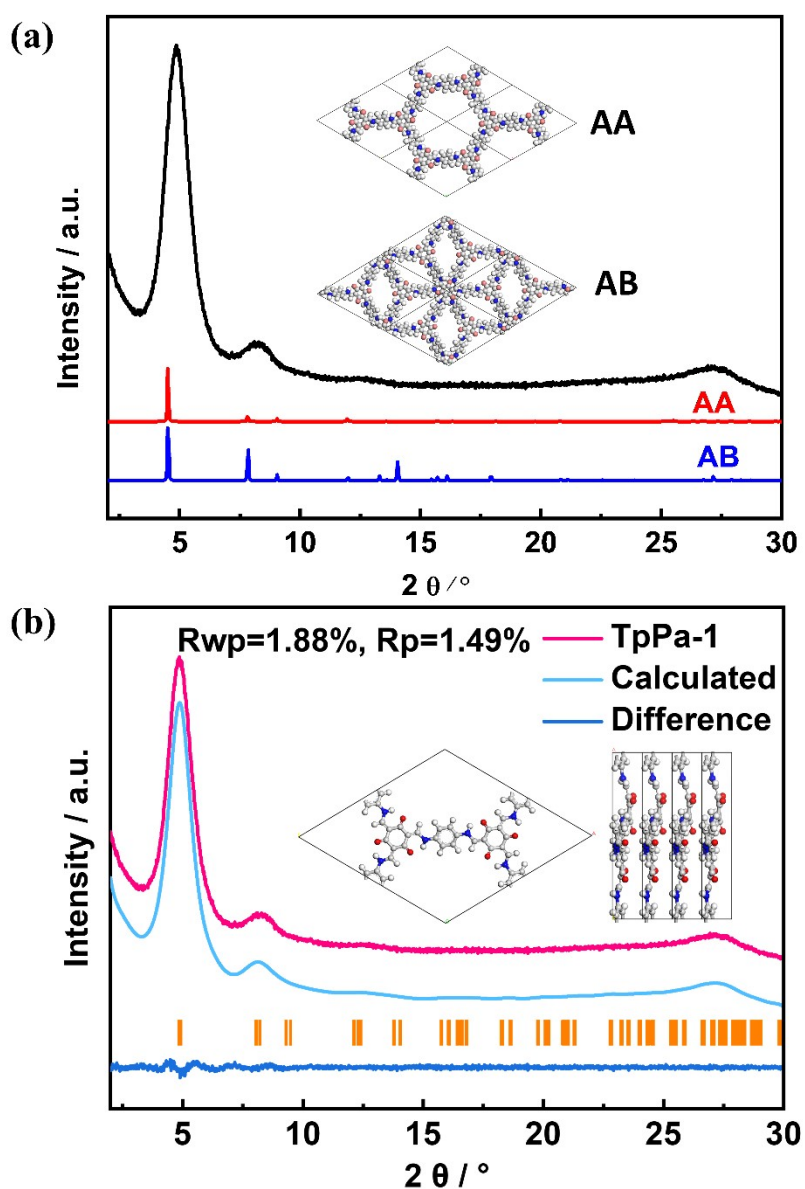


Figure S1. (a) PXR D patterns of the TpPa-1: experimentally observed (black), simulated using eclipsed AA-stacking (red), and staggered AB stacking (blue) models. Crystal structures of the

eclipsed AA stacking and staggered AB stacking model in the P3 space group. (b) comparison between the experimental and Pawley refined profiles. Inset: the crystal structures of corresponding.

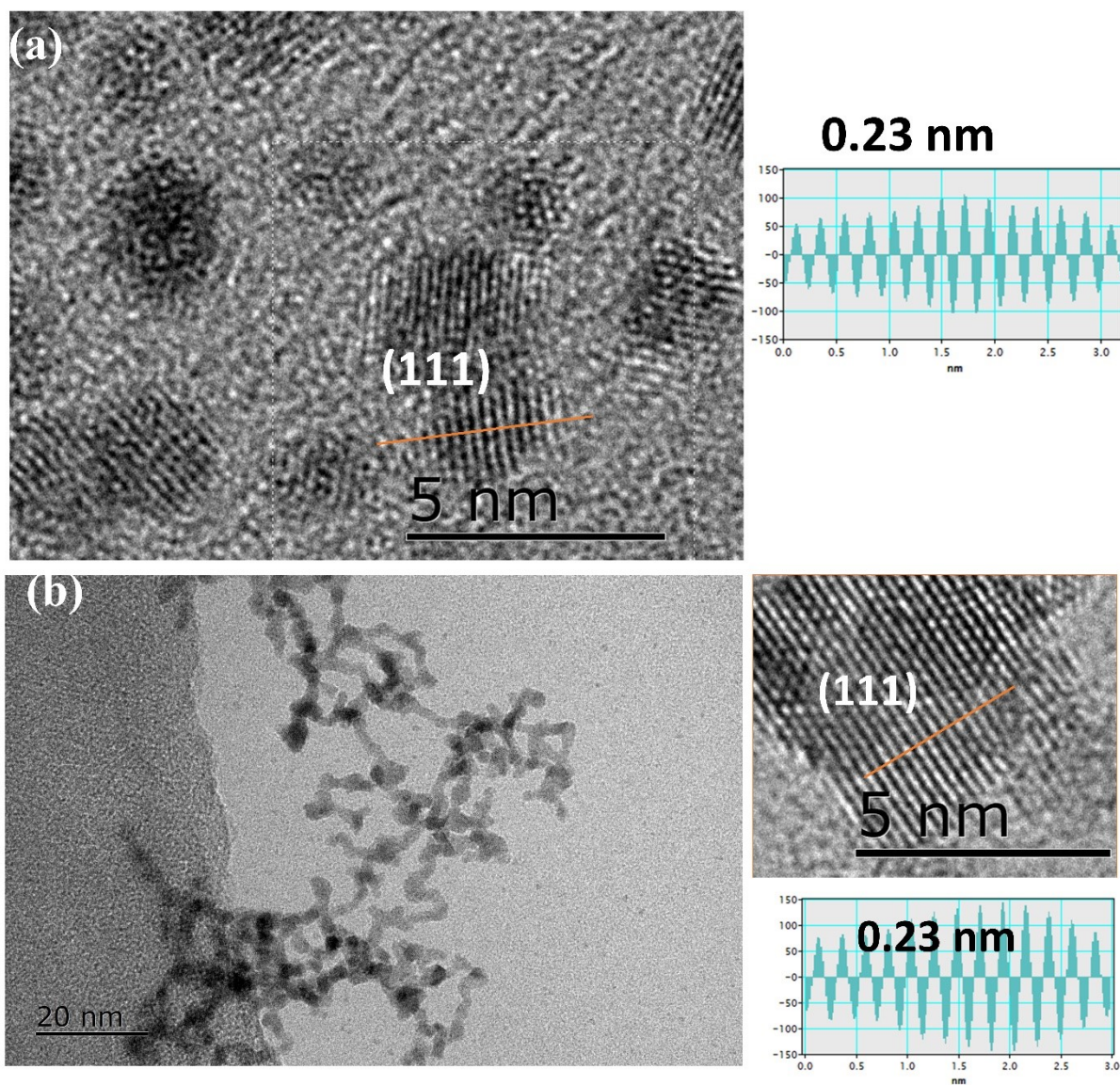


Figure S2. (a) HRTEM of SC-stabilized PtNPs; (b) The TEM image of PtNPs (115) and the corresponding HRTEM (Inset).

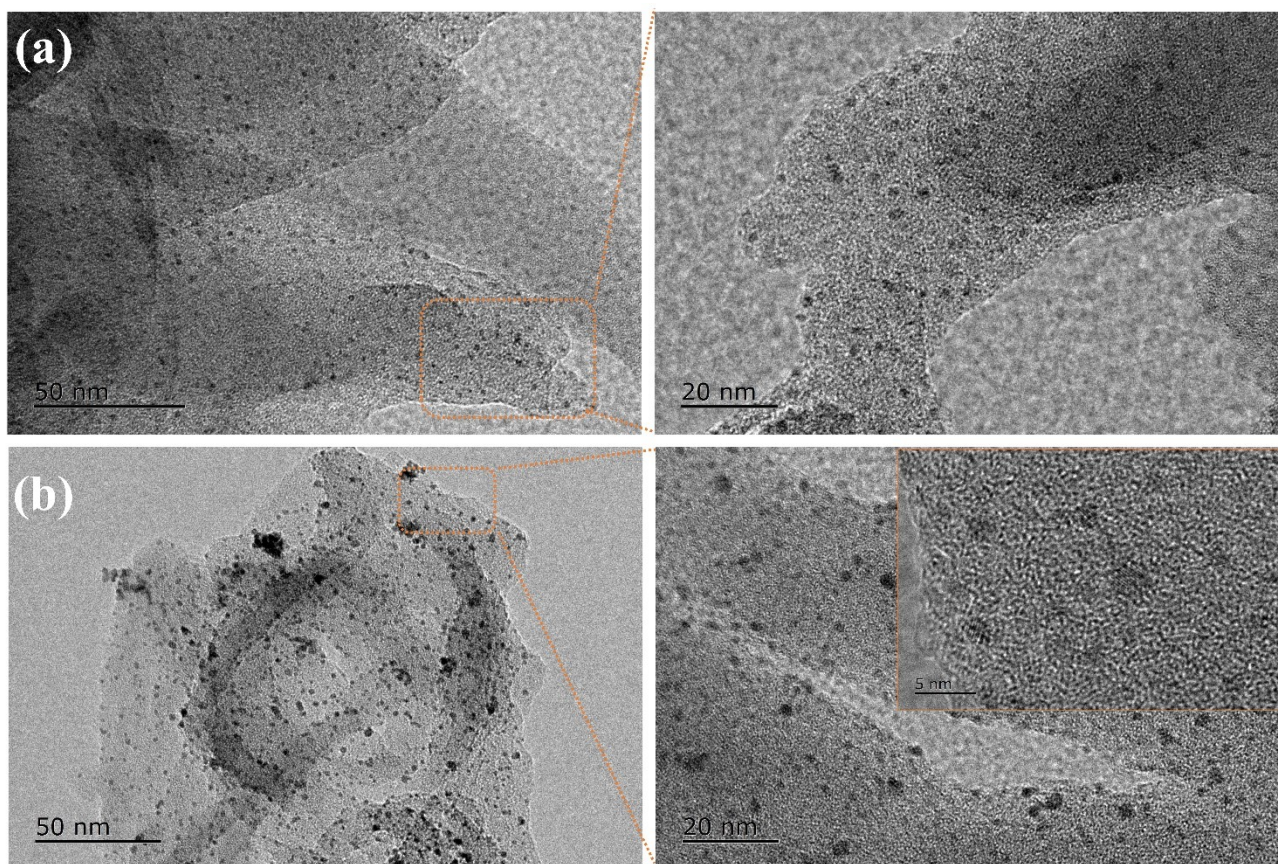


Figure S3. TEM images of (a) 0.5%PtNPs-TpPa-1; (b) 0.5%Pt-TpPa-1 and the corresponding enlarged images.

Table S1. Content of Pt in the samples.

Samples	Pt (mg/L)	Content of Pt (wt %)
TpPa-1	~0	~0
0.5%Pt-TpPa-1	0.51	0.51%
0.5%PtNPs-TpPa-1	0.49	0.49%

Pt amount in each sample was identified by Induced coupled plasma mass spectroscopy (ICP-MS) and Inductively coupled plasma optical emission spectrometer (ICP-OES) using Agilent 5110. Typically, 10 mg of the samples were dissolved in 10 ml aqua regia solution for 24 h. The solution was diluted 10 times by deionized water and filtrated to generate a transparent solution, which was used for the test by ICP-MS (TpPa-1) and ICP-OES (0.5%Pt-TpPa-1 and 0.5%PtNPs-TpPa-1). The quantification of the Pt content in each sample is listed in Table S1.

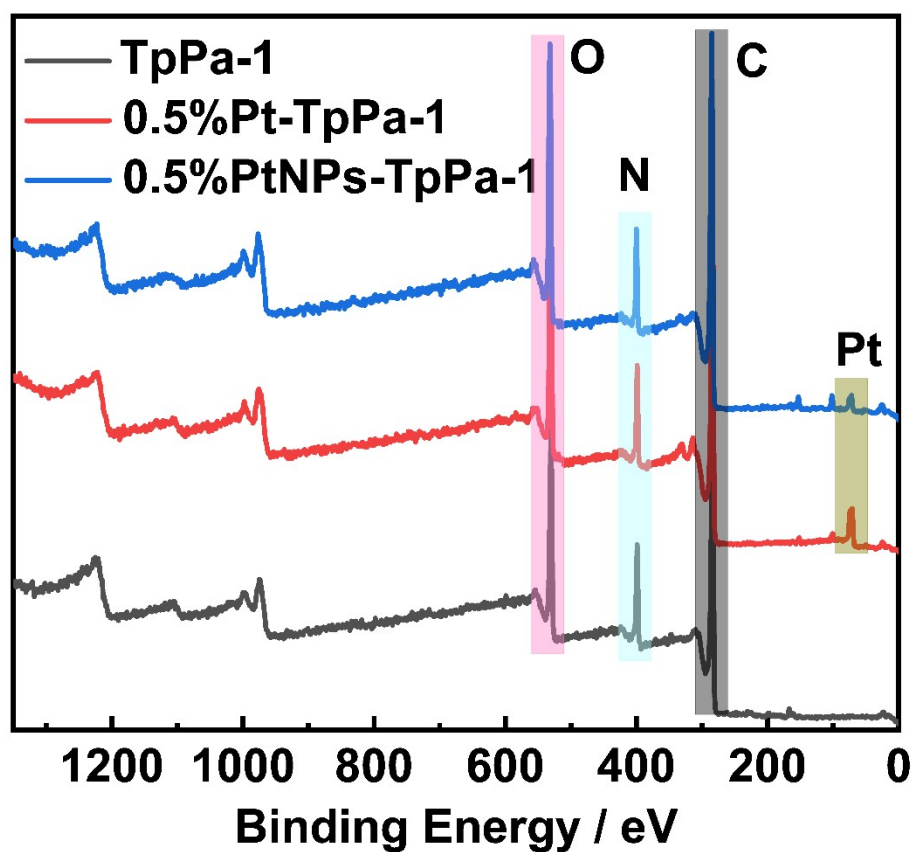


Figure S4. The XPS survey spectra of the samples.

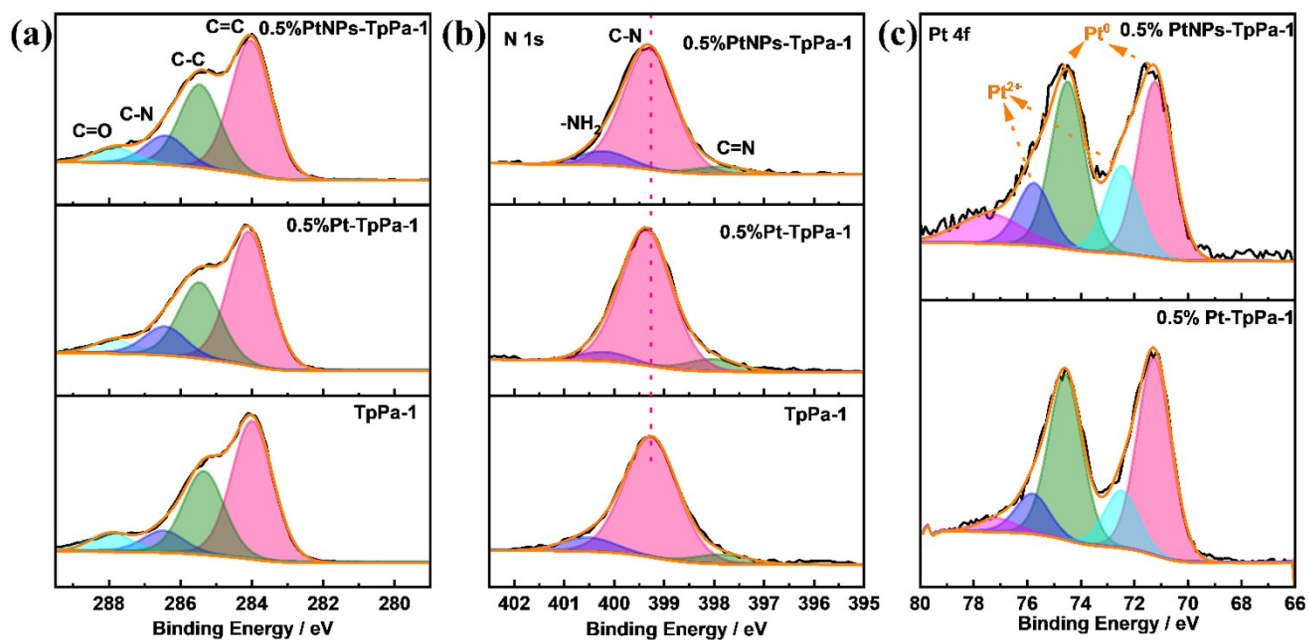


Figure S5. The high resolution XPS (a)O 1s, (b) N1s and (c) Pt 4f spectra of TpPa-1, 0.5%Pt-TpPa-1 and 0.5%PtNPs-TpPa-1.

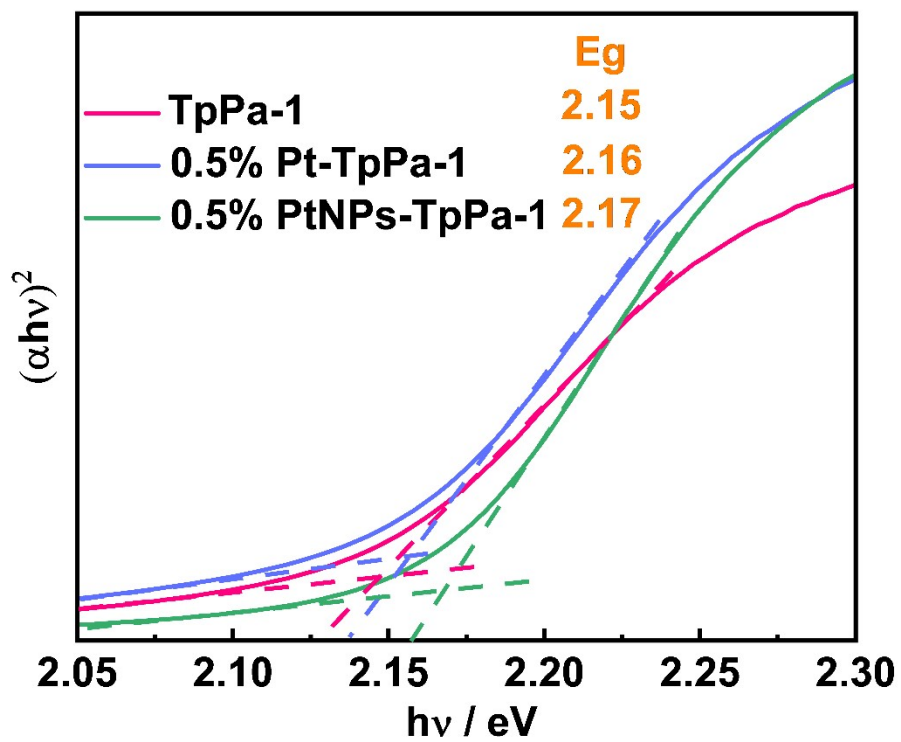


Figure S6. Tauc plots of the samples.

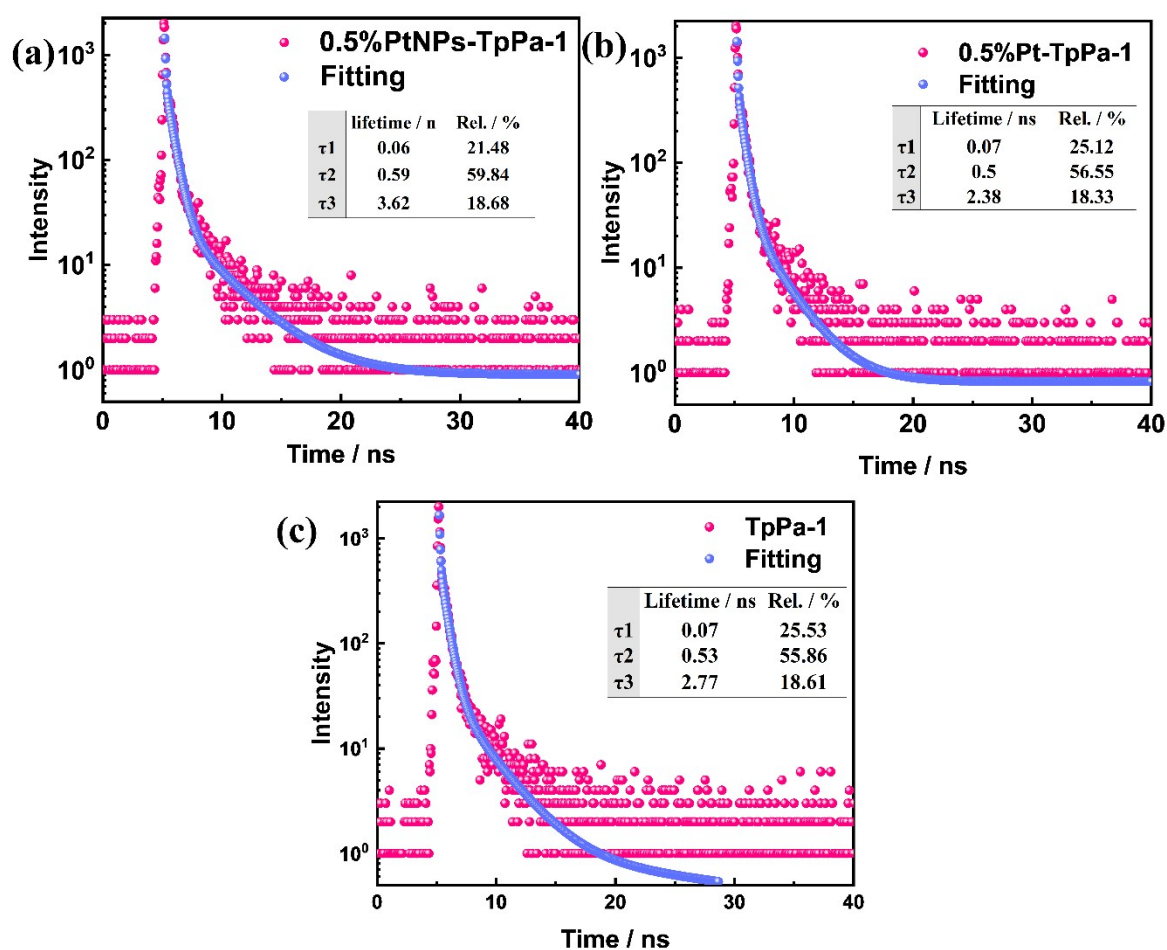


Figure S7. The fluorescence lifetimes of the samples.

Table S2. Apparent quantum Yield (AQY) of TpPa-1 COF-based photocatalysts coupled Pt co-catalyst for H₂ evolution.

COFs	Content of Pt (wt%)	AQY	Conditions	Reference
<i>0.5%PtNPs-TpPa-1</i>	<i>0.5% (PtNPs)</i>	<i>13.5% (450 nm)</i>	<i>AA $\lambda > 420$ nm</i>	<i>This work</i>
Pt-PVP-BT-COF	6% PVP-Pt	0.4% (475 nm)	AA $\lambda > 420$ nm	Angew. Chem. Int. Ed. 2019, 58, 8290–18294
TpPa-H	≈3%	< 3% (450 nm)	SA $\lambda > 420$ nm	Chem.Eng. J., 2021 , 419
WO ₃ @TpPa-1-COF/rGO (30%)	3%	12.08 % (450 nm)	SA $\lambda > 420$ nm	Chem. Eng. J., 2022 , 431
ATNT-4	3%	9.75%	AA	J. Am. Chem.

		(500 nm)	$\lambda > 420$ nm	Soc., 2020 , 142 (10): 4862-4871
TiO ₂ -TpPa-1-COF	3%	7.6% (420 nm)	SA $\lambda > 420$ nm	Appl. Catal. B: Environ., 2020 , 266: 118586
RC-COF-1	3%	6.39% (420 nm)	AA $\lambda > 420$ nm	Nature, 2022 , 604 (7904): 72-79.
3%Pt ₁ @TpPa-1	0.72%	0.38% (420 nm)	SA $\lambda > 420$ nm	ACS Catal. 2021 , 11 (21), 13266-13279.
MOF-808@TpPa-1-COF	3%	10.23% (450 nm)	SA $\lambda > 420$ nm	J. Mater. Chem. A, 2021, 9, 16743-16750

Notes: Ascorbic acid (AA), Sodium ascorbate (SA)

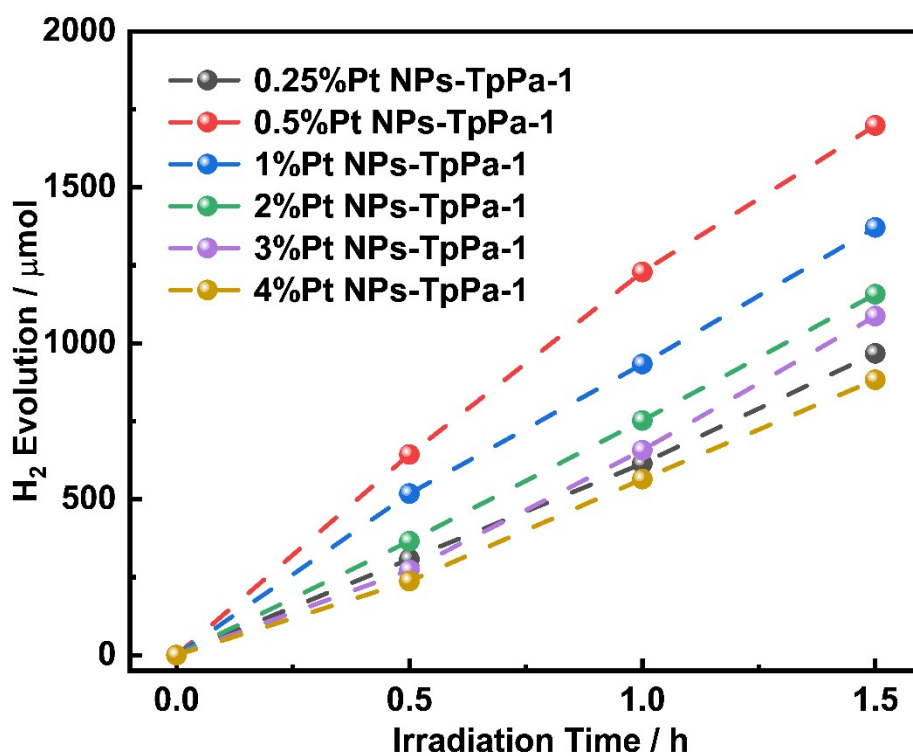


Figure S8. Time-dependent H₂ evolution for the samples with different SC-stabilized PtNPs loading using the pore encapsulation method.

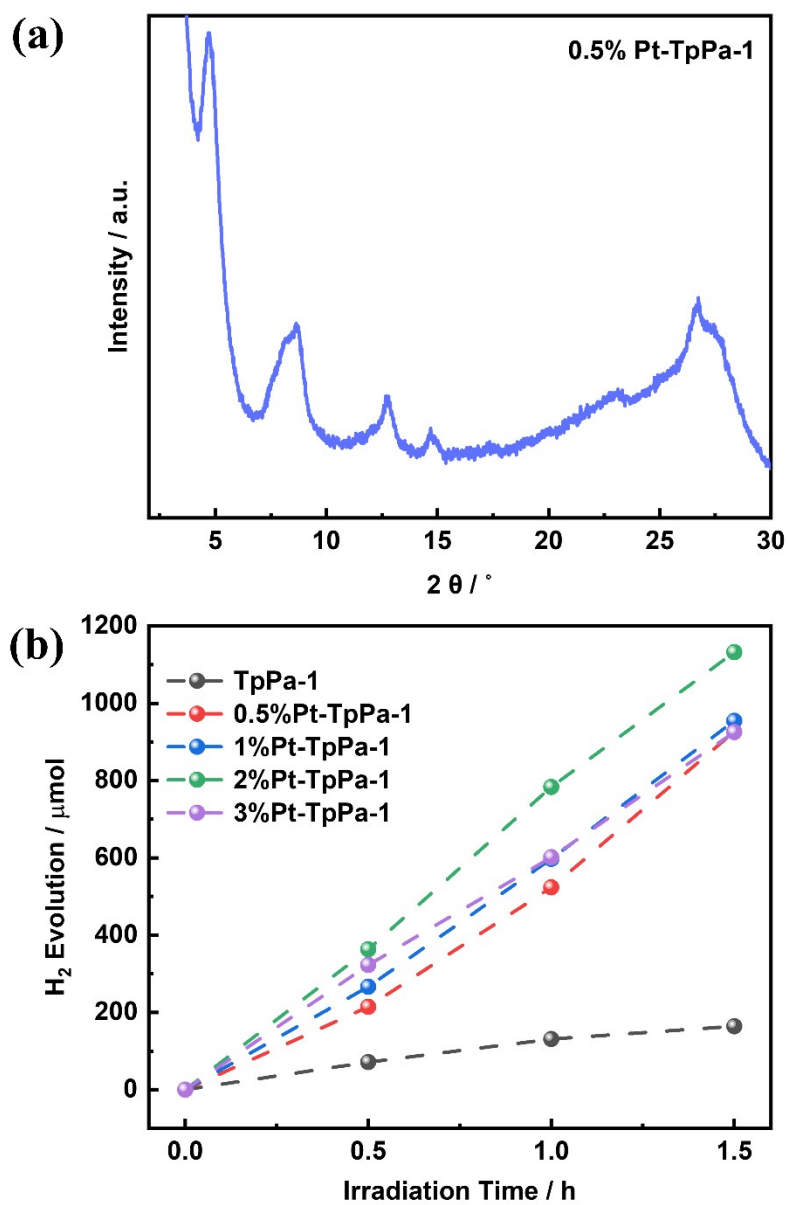


Figure S9. (a) The PXRD pattern of the 0.5%Pt-TpPa-1; (b) Time-dependent H₂ evolution for the samples with different Pt loading using photo-deposition method.

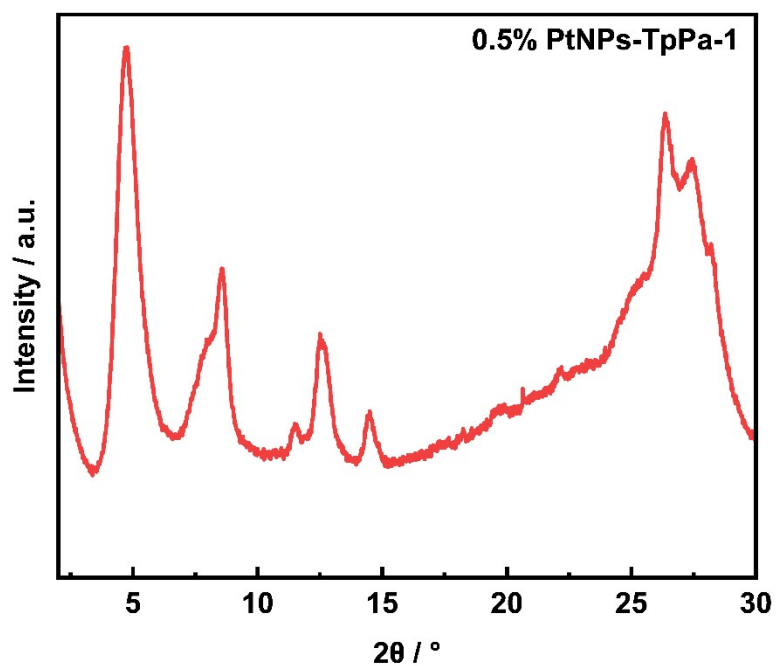


Figure S10. The PXRD pattern of the 0.5%PtNPs-TpPa-1 after the photocatalytic reaction.

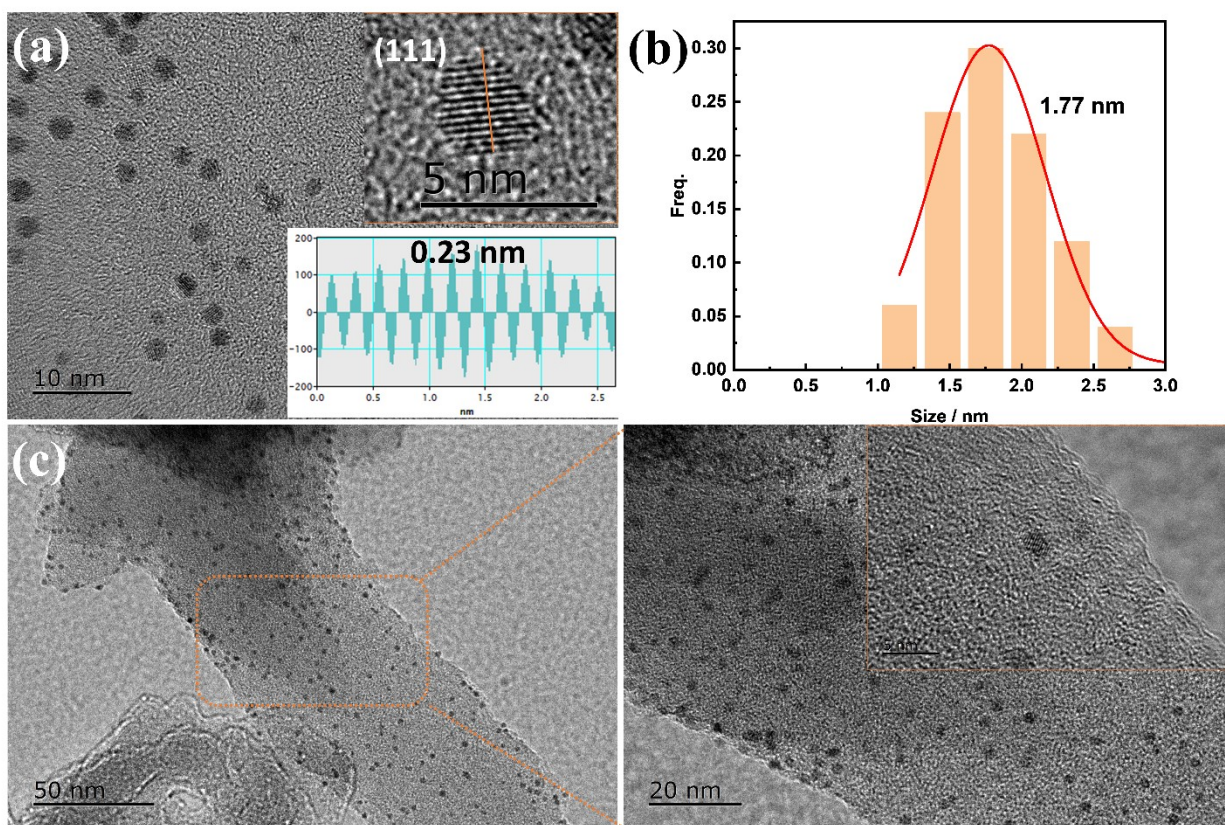


Figure S11. (a) TEM images of SNPs (PVP) and the corresponding HRTEM (the insets); (b) The size distribution of PtNPs (PVP); (c) 0.5%PtNPs(PVP)-TpPa-1 and the corresponding HRTEM (the insets).

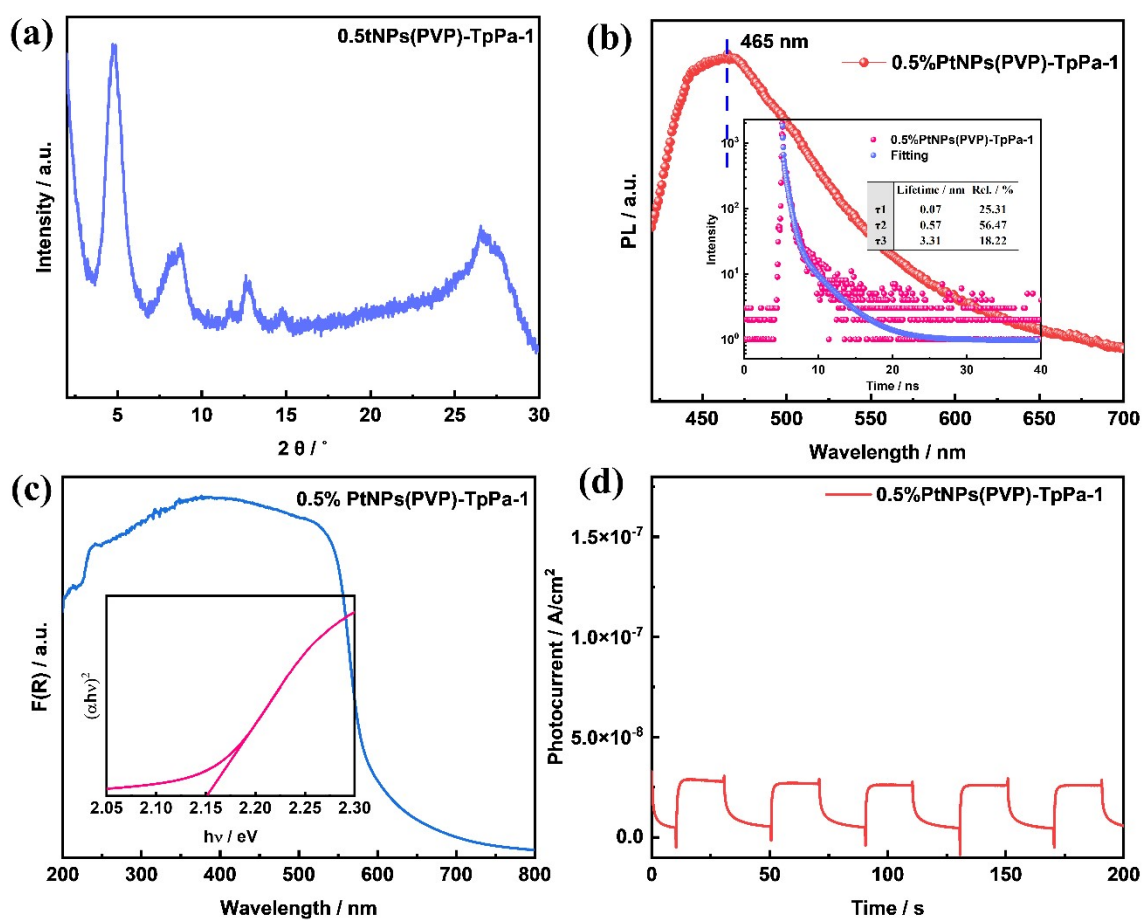


Figure S12. (a)PXRD; (b) PL and the fluorescence lifetime; (c) UV-Vis DRS spectrum and the Tauc plot; (d) Photocurrent test of 0.5%PtNPs(PVP)-TpPa-1.

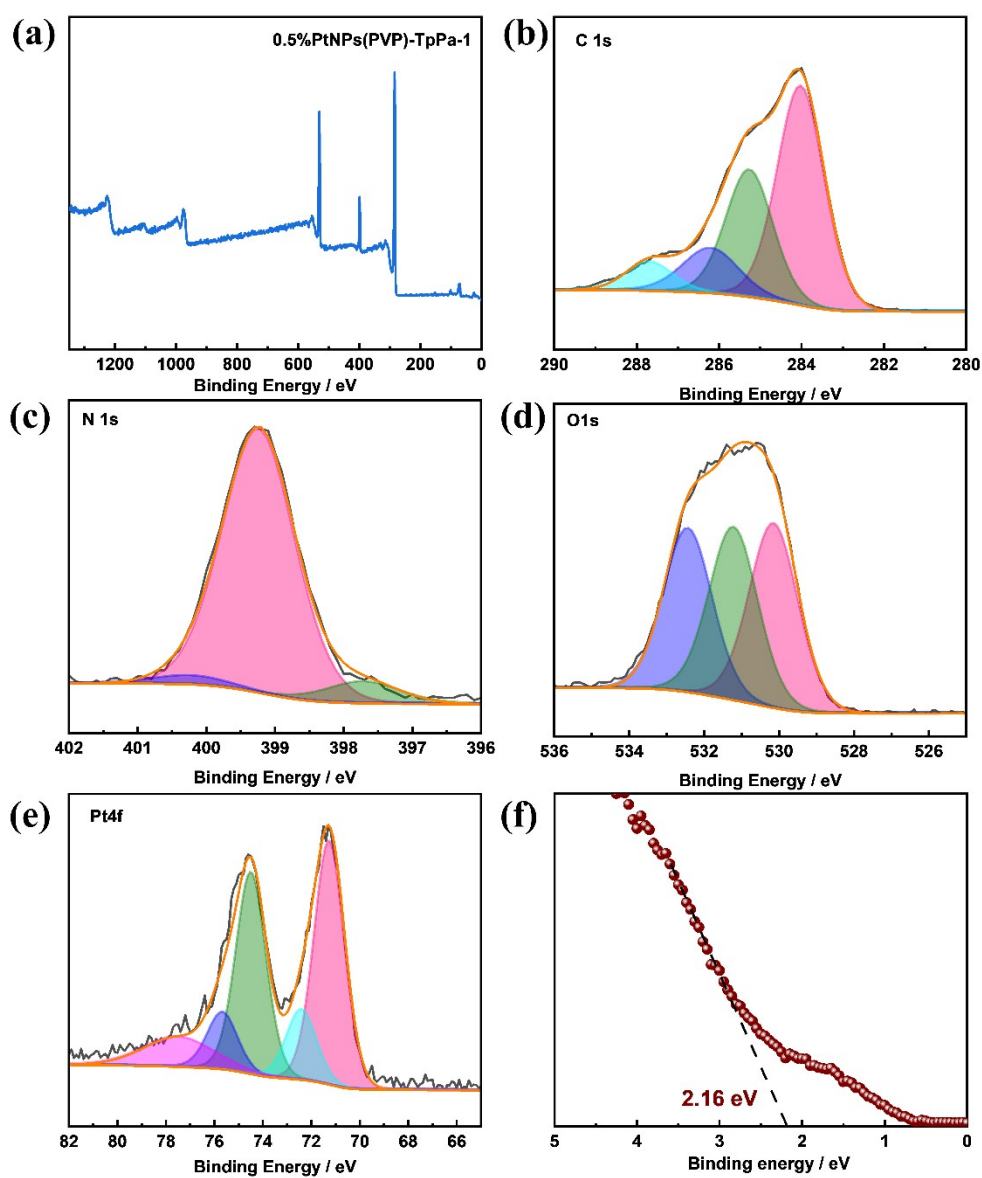


Figure S13. (a)The XPS survey spectra; The high-resolution XPS (b) C 1s (c) N1s (d) O 1s, and (e) Pt 4f spectra; (f) UPS spectrum of 0.5%PtNPs(PVP)-TpPa-1.

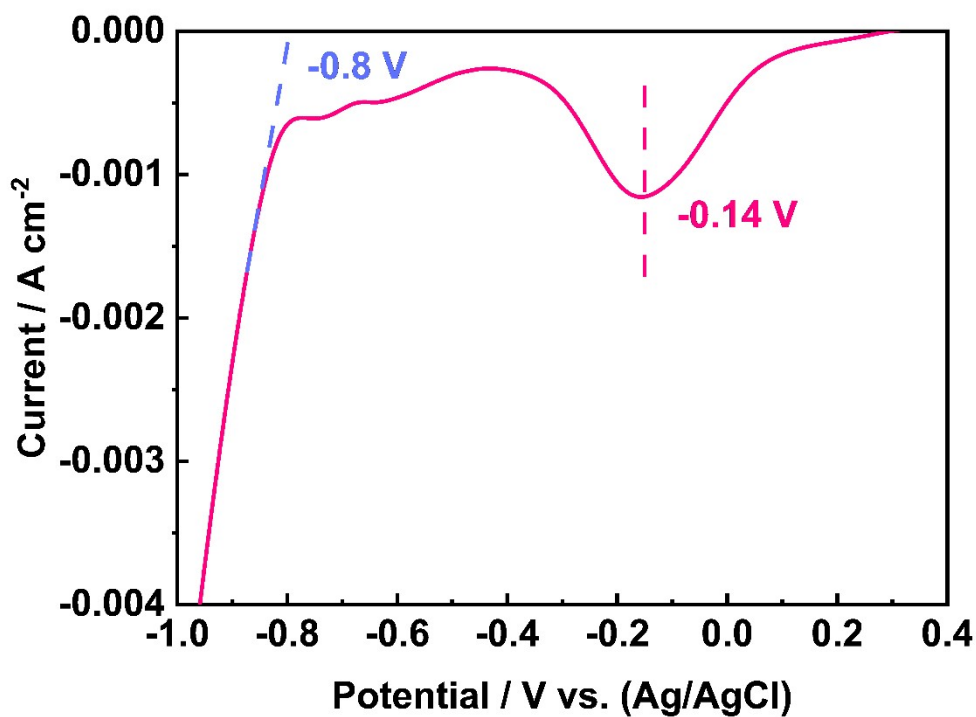


Figure S14. The LSV curve of Pt electrode in 1M SC aqueous solution.

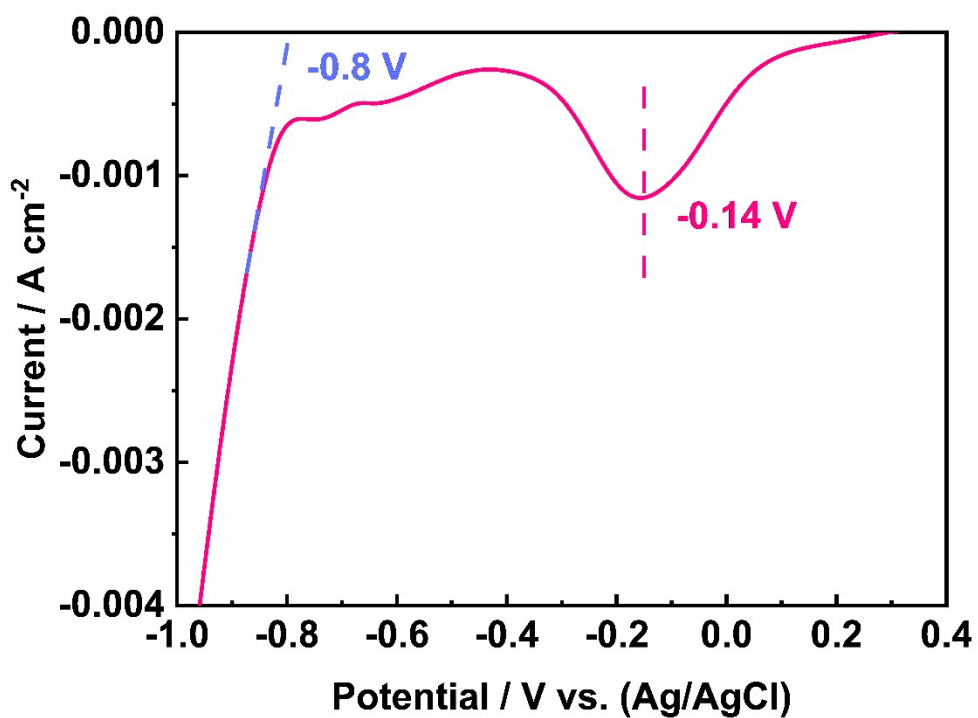


Figure S15. CV curve of SC aqueous solution (1 M) in air for 10 cycles.

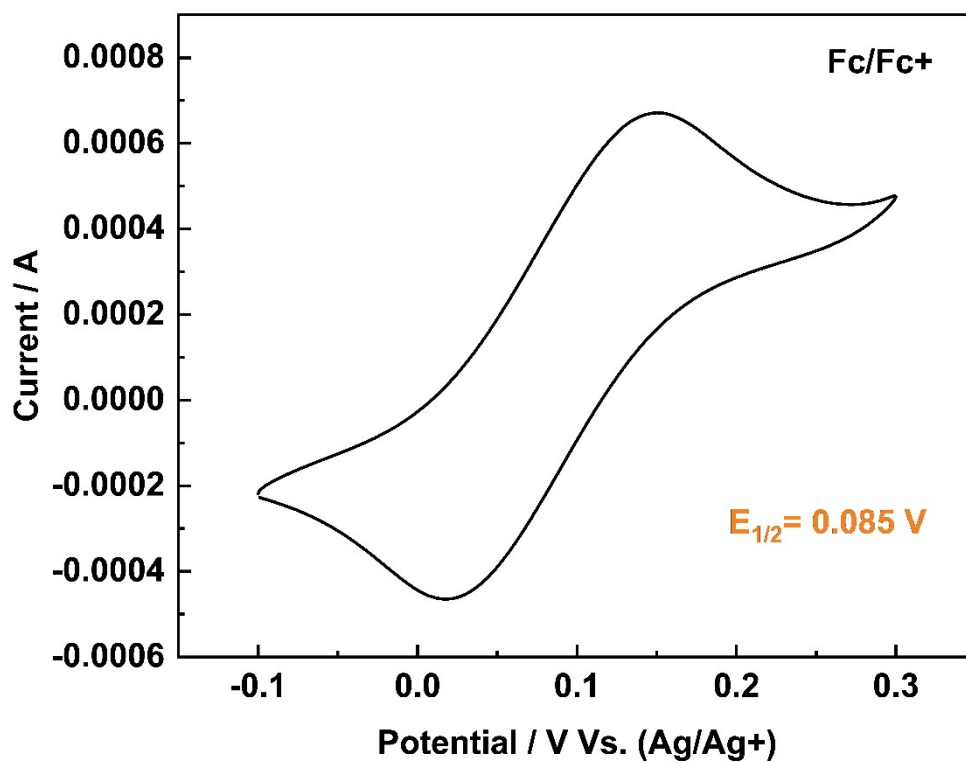


Figure S16. CV measurements of ferrocene/ferrocenium couple to calibrate the pseudo reference electrode.

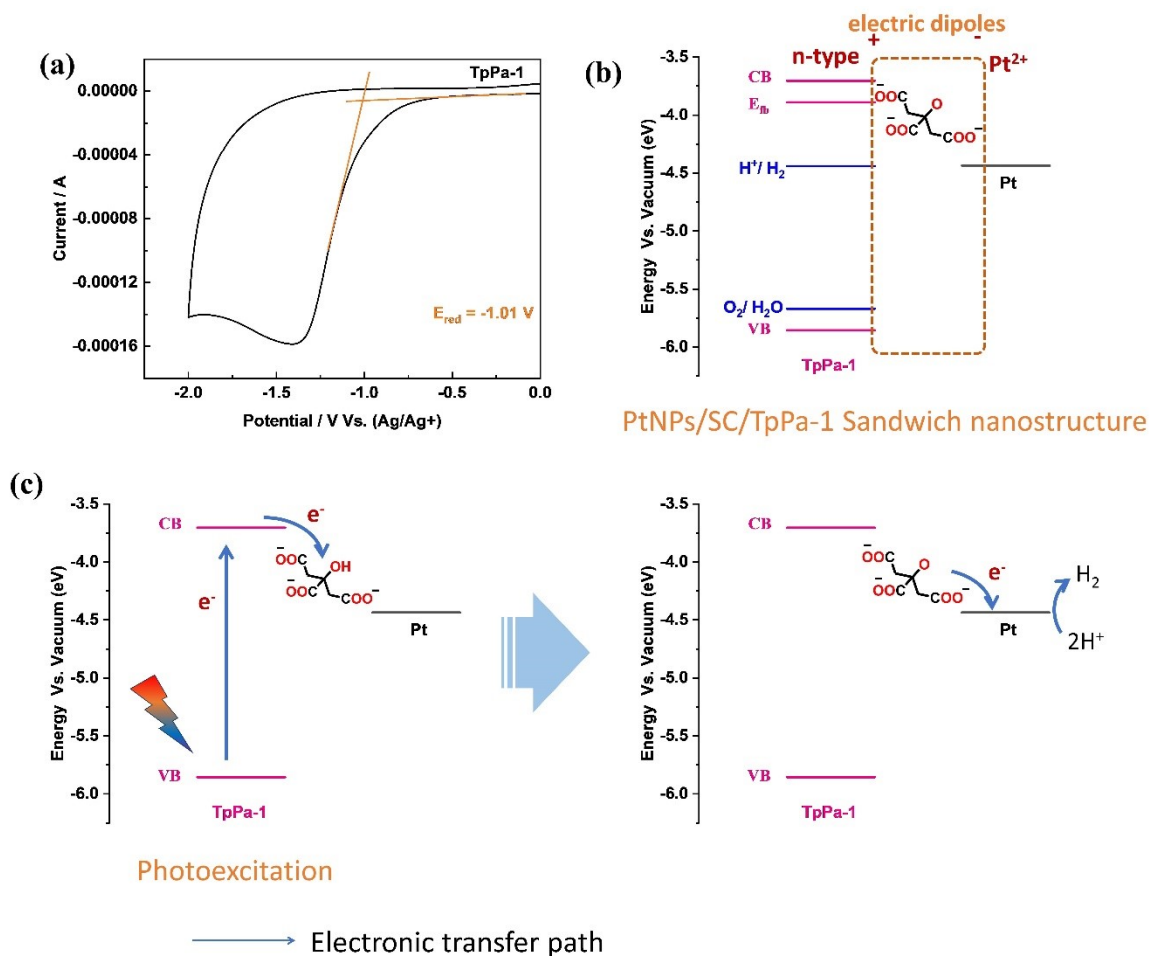


Figure S17. (a) The CV curve of TpPa-1; (b) Energy band of PtNPs/SC/TpPa-1 sandwich nanostructure; (c) Photogenerated electron transmission path.

TpPa-1 exhibited electronegativity due to it's a n-type organic semiconductor. The PtNPs presented electropositive because of the Pt²⁺ on the surface. Interfacial SC electron dipoles can be formed by the different charges at both ends (**Figure S17b**).

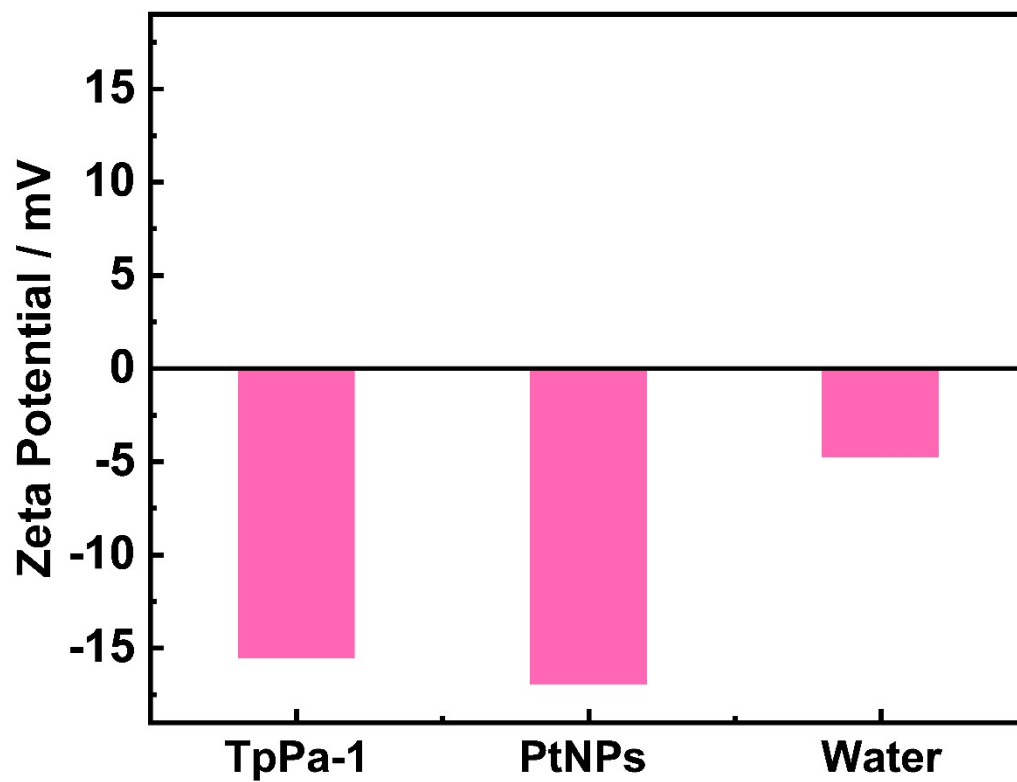


Figure S18. Zeta potentials of TpPa-1, SC stabilized PtNPs (110), and the deionized water.

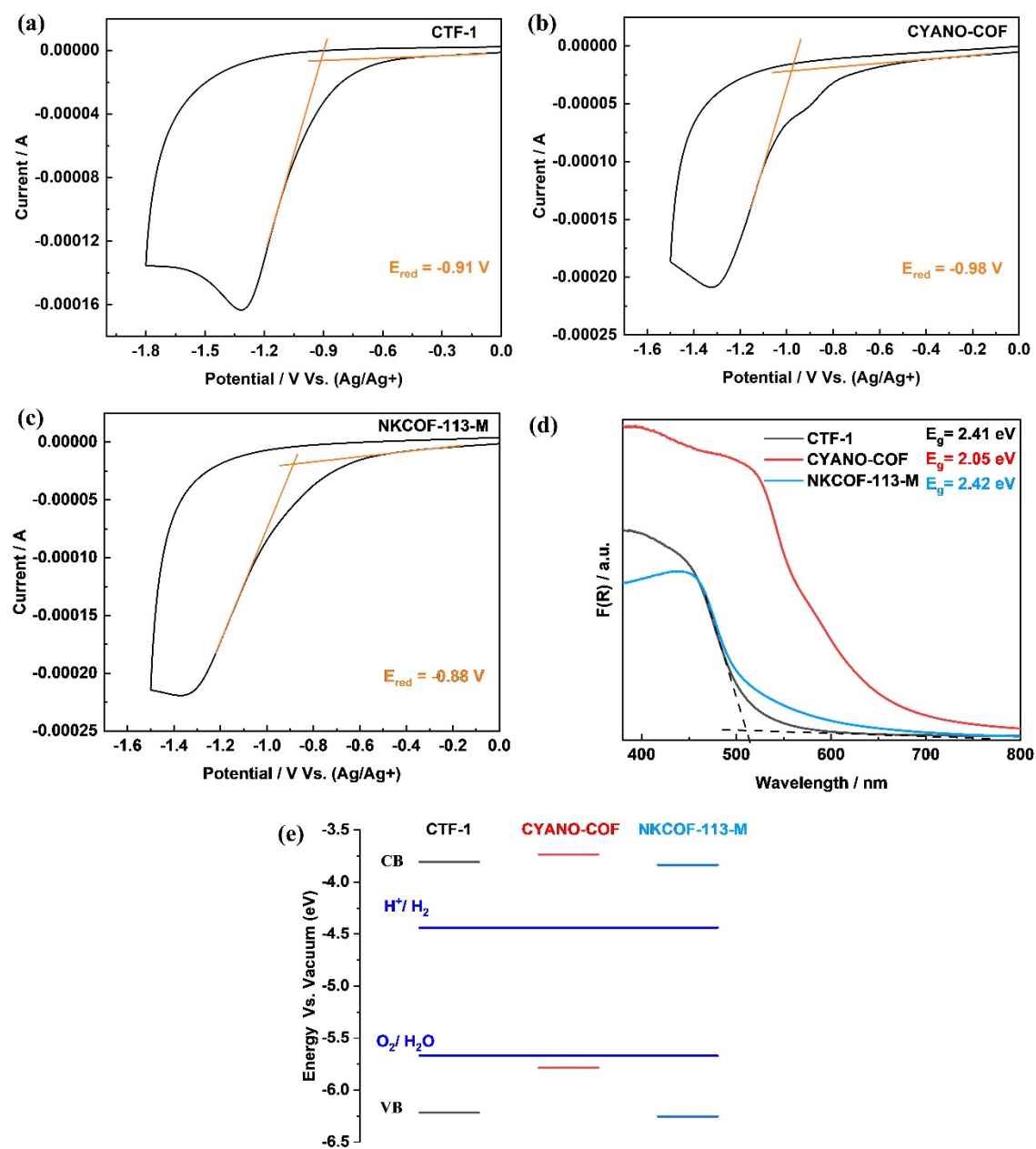


Figure S19. The CV curves of (a) CTF-1, (b) CYANO-COF, and (c) NKCOF-113-M; (d) The DRS of the samples; (e) The energy band structure of the samples.

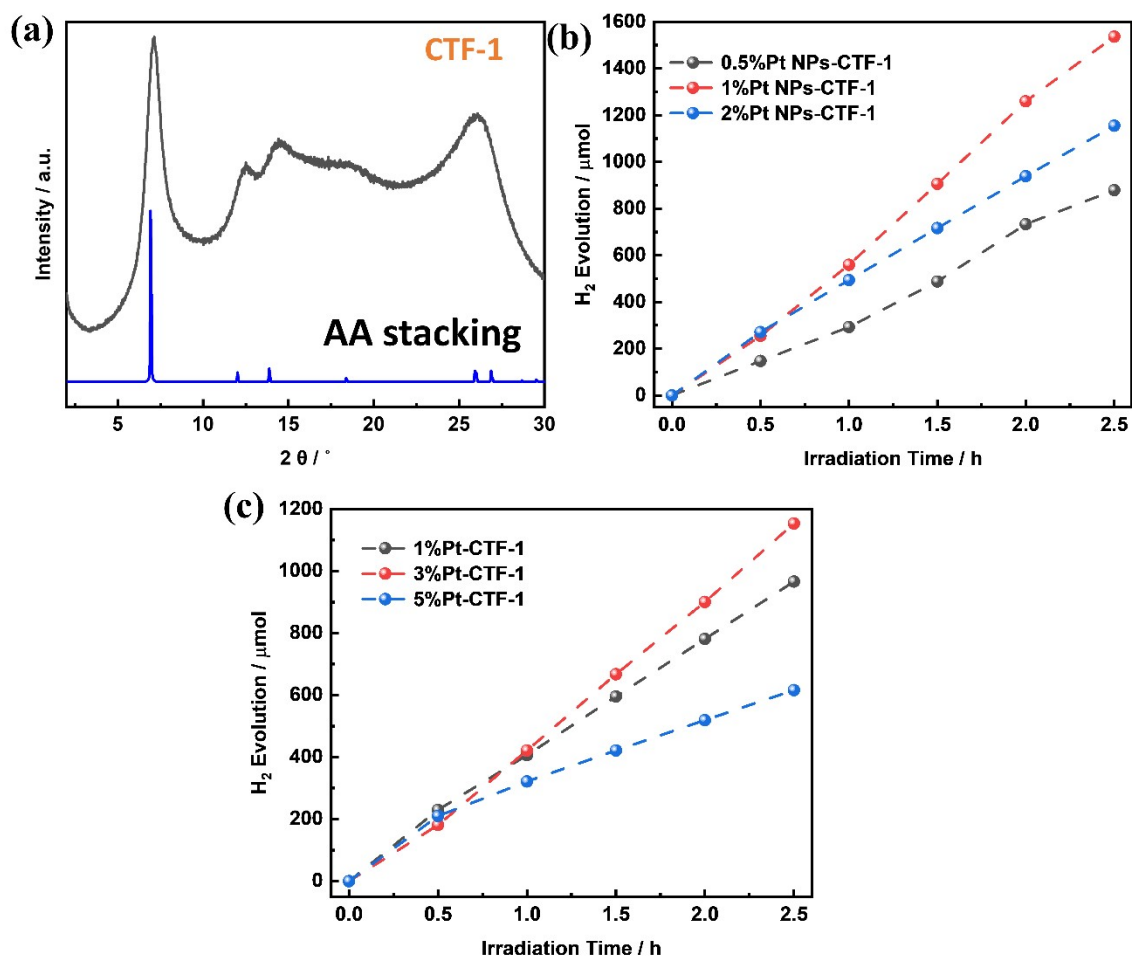


Figure S20. (a) PXRD patterns of CTF-1. (b) Time-dependent H₂ evolution for the samples with different SC stabilized PtNPs loading. (c) Time-dependent H₂ evolution for the samples with different Pt loading by photo-deposition.

After optimization of PtNPs loading capacity, 1%PtNPs-CTF-1 showed the largest photocatalytic H₂ evolution rate of ~630 μmol/h. Compared to this, the optimal Pt loading for the photo-deposition method is 3 wt %, and its H₂ evolution rate is only ~470 μmol/h.

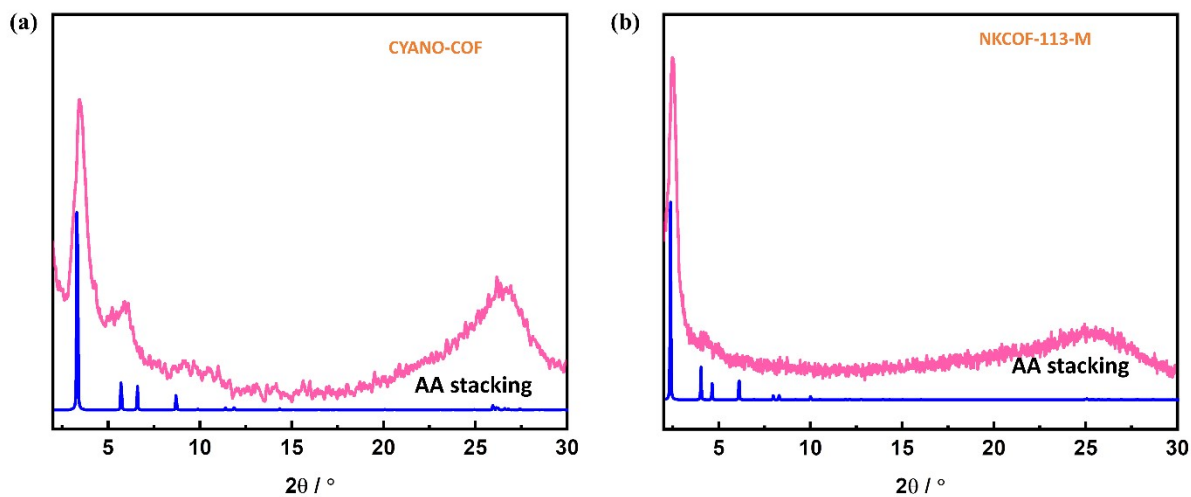


Figure S21. PXRD patterns of (a) CYANO-COF and (b) NKCOF-113-M.

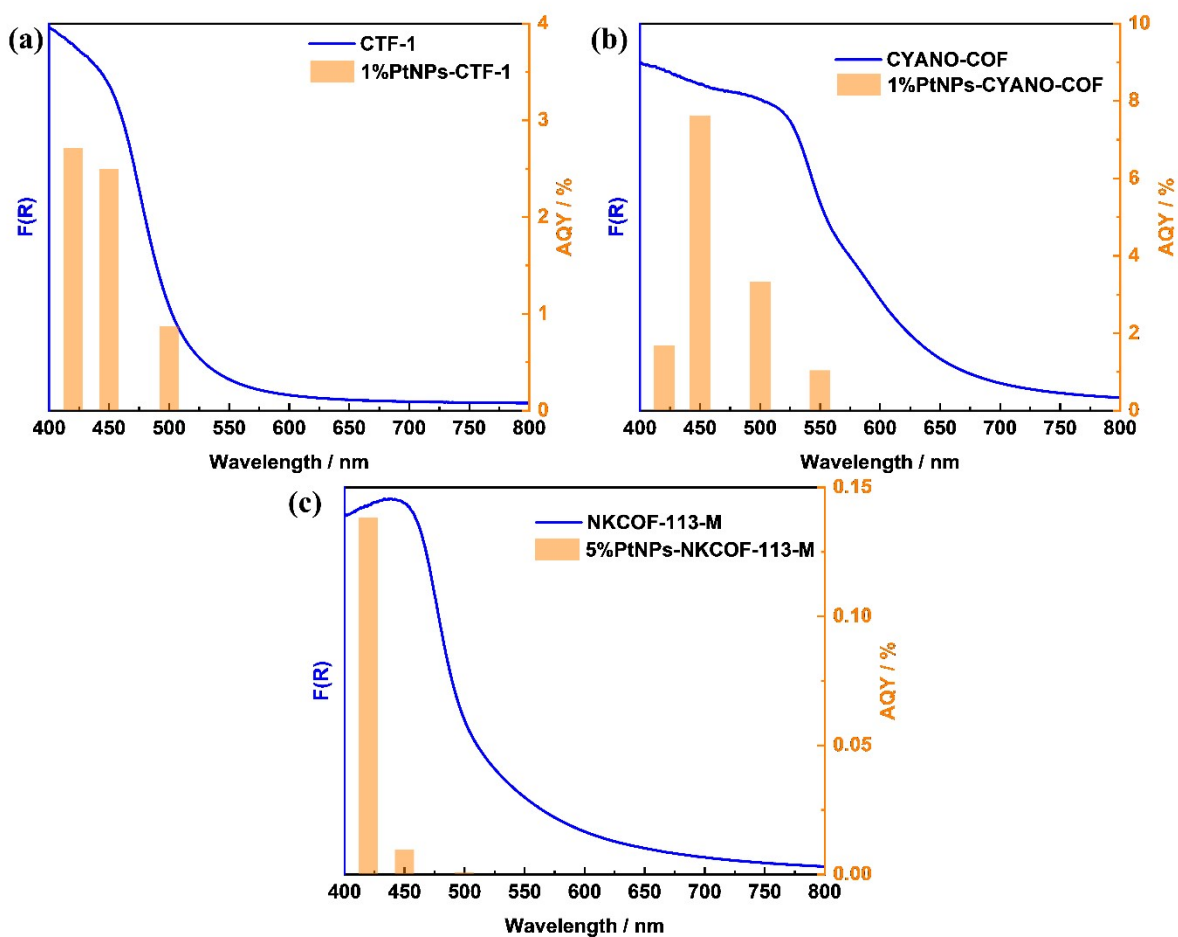


Figure S22. The photocatalytic HER AQY of (a) 1%PtNPs-CTF-1, (b) 1%PtNPs-CYANO-COF, and (c) 5%PtNPs-NKCOF-113-M.

Table S3

References

1. C. Wang, H. Zhang, W. Luo, T. Sun and Y. Xu, *Angew. Chem. Int. Ed.*, 2021, **60**, 25381-25390.
2. C. Li, J. Liu, H. Li, K. Wu, J. Wang and Q. Yang, *Nat. Commun.*, 2022, **13**, 2357.
3. Z. Zhao, X. Chen, B. Li, S. Zhao, L. Niu, Z. Zhang and Y. Chen, *Adv. Sci.*, 2022, DOI: 10.1002/advs.202203832, e2203832.
4. M. Xu, D. Li, K. Sun, L. Jiao, C. Xie, C. Ding and H. L. Jiang, *Angew. Chem. Int. Ed.*, 2021, **60**, 16372-16376.
5. J. Pommerehne, H. Vestweber, W. Guss, R. F. Mahrt, H. Bässler, M. Porsch and J. Daub, *Adv. Mater.*, 1995, **7**, 551-554.
6. Q. Sun, H. Wang, C. Yang and Y. Li, *J. Mater. Chem.*, 2003, **13**, 800-806.
7. H. Eckhardt, L. W. Shacklette, K. Y. Jen and R. L. Elsenbaumer, *J. Chem. Phys.*, 1989, **91**, 1303-1315.